# Segmentation of Pigmented Skin Lesions Using Non-negative Matrix Factorization

Pablo G. Cavalcanti, Jacob Scharcanski[▲]
Instituto de Informática
Universidade Federal do Rio Grande do Sul
Porto Alegre, Brazil
[▲]jacobs@inf.ufrgs.br

César E. Martínez, Leandro E. Di Persia[*]
Research Center for Signals, Sytems
and Computational Intelligence (SINC)
Facultad de Ingeniería, Universidad Nacional del Litoral
[*]ldipersia@fich.unl.edu.ar

***Abstract*—Melanoma is a type of malignant pigmented skin lesion, which currently is among the most dangerous existing cancers. Segmentation is an important step in computer-aided pre-screening systems for pigmented skin lesions, because a good definition of the lesion area and its rim is very important for discriminating between benign and malignant cases. In this paper, we propose to segment pigmented skin lesions using the Non-negative Matrix Factorization of the multi-channel skin lesion image representation. Our preliminary experimental results on a publicly available dataset suggest that our method obtains lower segmentation errors (in average) than comparable state-of-the-art methods proposed in literature.**

sinc(*i*) Research Center for Signals, Systems and Computational Intelligence (fich.unl.edu.ar/sinc)
P. Cavalcanti, J. Scharcanski, C. E. Martínez & L. Di Persia; "Segmentation of pigmented skin lesions using Non-negative Matrix Factorization"
In Instrumentation and Measurement Technology Conference (I2MTC) Proceedings, pp. 72-75, may, 2014.

## I. Introduction

The efforts to use computer-based pre-screening tools in pigmented skin lesions started nearly 30 years ago. It is possible to find teledermatology systems in the literature enabling experts to receive images captured remotely of suspicious lesions with a diagnosis indication; computer-aided pre-screening systems that classify an acquired lesion image; and hybrid systems that use telemedicine and computer-aided pre-screening in conjunction [1]. According to World Healthy Organization [2], about 132000 melanoma cases occur globally each year. The current high incidence of malignant melanoma, a dangerous kind of pigmented skin lesion, motivates researchers to propose new developments in this area.

Discriminating malignant (melanomas) and benign pigmented skin lesions (e.g. nevi or moles) can be challenging. Usually, dermatologists screen each lesion with a dermoscope, a noninvasive tool that magnifies morphologic and vascular lesion structures. Therefore, many pre-screening systems have been proposed to help physicians analyze dermoscopy images [3], [4], [5]. However, considering that a dermoscope is a specialized tool, pre-screening systems dealing with standard camera images (i.e. simple photographs) also have been proposed in an attempt to provide easy access to health-care. Consequently, even non-specialized systems running on mobile devices (e.g. smartphones) have been proposed [6]. Although these non-specialized systems are not designed to replace the specialists, they still can be used in practice for pre-screening (i.e., in a filtering or triage step), helping establish a priority in the assignment of skin lesion patients to specialists [6].

In general, a pre-screening system has four stages: (a) preprocessing: where the image artifacts are eliminated to facilitate the segmentation step; (b) segmentation: where the lesion rim is delimited; (c) feature extraction: where a quantitative description of the lesion is generated based on the lesion segment; and (d) classification, where the lesion features are identified as benign or malignant. As can be seen, it is a sequential scheme, and each step depends on the previous one. This explains why the first two steps receive ample attention in the literature, and also are the focus of this work.

Standard camera images of pigmented skin lesions usually contain shading areas, which may be wrongly segmented as lesion in the segmentation step if not attenuated during preprocessing. Some authors also eliminate hair in this step, often with the DullRazor algorithm [7]. However, it has been observed [8] that hair can be eliminated easily in the post-processing stage. Alcón et al. [9] proposed to attenuate shading by removing low frequency spatial components of the skin lesion image. However, it requires to specify parameters that are difficult to obtain for any input image. So, in this work, as we detail in Section II, we use the Cavalcanti et al. [8] shading attenuation method, which is adaptive and fully automatic.

Several schemes have been used for segmenting pigmented skin lesions on standard camera images, applied to grayscale images [10], [11], [12] or to the Red channel (i.e., R of the RGB color space) [13]. Alcón et al. method [9] determines the healthy skin pixels assuming that their grayscale histogram follows a Gaussian-like distribution. The method proposed by Tang [14] smooths the image with an adaptive anisotropic diffusion filter, and then uses a modification of the Gradient Vector Flow snake [15] to determine the lesion rim. Cavalcanti and Scharcanski [8] use the Otsu's thresholding method [16] on a multi-channel image representation (see Section III). Also, Cavalcanti et al. [17] proposed to use Independent Component Analysis (ICA) to provide an initialization, and then segment the pigmented skin lesion in an input image using the Chan-Vese active-contours method [18]. With the exception of Alcón et al. method, all above mentioned segmentation methods require a post-processing stage based on morphological operations to eliminate possible artifacts, and/or to refine the lesion rim.

The remaining of this paper is organized as follows. In Section III we present our proposed segmentation method, which is compared with state-of-art segmentation methods in Section IV. Finally, we present our conclusions in Section V.

978-1-4673-6386-0/14/$31.00 ©2014 IEEE

## II. PREPROCESSING

As mentioned above, we use the shading attenuation method proposed by Cavalcanti and Scharcanski [8], which was designed specifically for pigmented skin lesions standard images.

The first step is to convert the image from the original RGB color space to the HSV color space, and retain the Value channel $V$. This is justified by the fact that in this channel the shading effects are more visible. We extract $20 \times 20$ pixels in each $V$ corner (regions usually containing only healthy skin pixels) and define $S$ as the union of these four sets. This pixel set is used to adjust the quadric function $z(x,y) = P_1x^2 + P_2y^2 + P_3xy + P_4x + P_5y + P_6$, where the six quadric function parameters $P_i$ $(i = 1, ..., 6)$ are chosen to minimize the squared error summation in the 1600 pixels of $S$.

After the calculation of the quadric function $z(x,y)$ for each image spatial location $(x,y)$, we have an estimate $z(x,y)$ of the local illumination intensity in the image $V(x,y)$. By dividing the original $V(x,y)$ channel by $z(x,y)$, we obtain a new Value channel where the shading effects have been attenuated. The final step is to replace the original Value channel by this new Value channel, and convert the image from the HSV color space to the original RGB color space.

## III. THE PROPOSED SEGMENTATION METHOD

Cavalcanti and Scharcanski [8] recently proposed a multichannel image representation for pigmented skin lesion images that maximizes the discrimination between healthy and unhealthy skin regions. Instead of using the original color image as input to the segmentation method, a 3-channel image representation $\bar{I}_i^N$ is used as input, as detailed next.

The first channel is a representation of the image darkness, relying on the fact that lesion areas are depigmented skin regions. Each pixel is defined as $\bar{I}_1^N(x,y) = 1 - \bar{I}_1^C(x,y)$, i.e. the complement of the normalized Red channel, where $\bar{I}_i^C$ are the normalized RGB channels (i.e., $\bar{I}_i^C(x,y) \in [0,1]$).

The second channel is a texture representation, since local textural variability usually is higher in lesions than in healthy skin areas. Being $\bar{L}$ a normalized Luminance image defined by the average of the three $\bar{I}_i^C$ channels at each pixel $(x,y)$, we quantify the textural variability in $\bar{L}(x,y)$ by computing $\tau(x,y,\sigma)$:

$$\tau(x,y,\sigma) = \bar{L}(x,y)\frac{\widetilde{S}(x,y,\sigma)}{S(x,y,\sigma)}, \quad (1)$$

where, $S(x,y,\sigma) = \bar{L}(x,y) * G(\sigma)$ (i.e., denotes the Luminance image $\bar{L}$ smoothed by a Gaussian filter with standard deviation $\sigma$), and $\widetilde{S}(x,y,\sigma)$ represents its complement. In this way, if an image region is dark, its textural information is emphasized; if the region is bright, its textural information is de-emphasized. However, a single Gaussian filter may not be sufficient to capture the textural variability, so $\tau(x,y,\sigma)$ is calculated for different $\sigma$ values and we select the maximum $T(x,y)$ value at each pixel. Finally, the texture variation channel $T$ is normalized, obtaining $\bar{I}_2^N(x,y) = (T(x,y) - \min(T)) \ / \ (\max(T) - \min(T))$.

The third channel $\bar{I}_3^N(x,y)$ of the representation describes the local color variation, assuming that healthy and unhealthy skin regions present different color distributions. The Principal Component Analysis (PCA) method is applied on the normalized colors of the image $\bar{I}_i^C(x,y)$, and the first component is retained (i.e. the component that maximizes the local data variance). Since the input data is centered around the mean, and healthy skin pixels often are more frequent in the image, the projections of the healthy skin pixels on the PCA space tend to generate values nearer to zero than the lesion pixels (i.e., the projected lesion pixels tend to have larger magnitudes, i.e. positive or negative). Therefore, the color variability information $C$ is represented by the pixel projection magnitudes, and the normalization of $C$ generates the $\bar{I}_3^N(x,y) = (C(x,y) - \min(C)) \ / \ (\max(C) - \min(C))$. Also, the $\bar{I}_3^N$ channel is filtered with a $5 \times 5$ median filter to reduce the noise.

Obtained this multichannel representation, we use the Non-negative Matrix Factorization (NMF) to segment the lesion image. The NMF is a recently proposed linear matrix factorization technique, which is intended to decompose a given non-negative matrix into two new matrices [19]. Let us consider $U$ samples of dimension $Q$, forming the non-negative matrix $\mathbf{Y} \in \mathbb{R}^{Q \times U}$. Through this decomposition we obtain : (a) two matrices that also are non-negative; and (b) have a smaller rank than $Y$. Thus, the method achieves an approximation to the signal in terms of a dictionary and activation coefficients, both being non-negative, which allows a better interpretation of the whole information when compared to related techniques such as Singular Value Decomposition and Independent/Principal Component Analysis.

The NMF model is given by:

$$\mathbf{Y} = \mathbf{AX} + \mathbf{E}; \quad \mathbf{A} \geq \mathbf{0}, \mathbf{X} \geq \mathbf{0}, \quad (2)$$

where $\mathbf{Y} \in \mathbb{R}^{Q \times U}$ is the observation matrix factorized by the bases matrix $\mathbf{A} \in \mathbb{R}^{Q \times R}$, and the contributions of each basis vector is given by $\mathbf{X} \in \mathbb{R}^{R \times U}$. The restriction of reduced rank is imposed by $R \leq \min(Q,U)$. The approximation error is given by the matrix $\mathbf{E} \in \mathbb{R}^{Q \times U}$. The estimation of the elements of $\mathbf{A}$ and $\mathbf{X}$ can be obtained by minimizing the distance (i.e., the Frobenius norm):

$$D_F(\mathbf{Y}||\mathbf{AX}) = \frac{1}{2}\|\mathbf{Y} - \mathbf{AX}\|_F^2, \quad (3)$$

subject to $a_{qr} \geq 0, x_{ru} \geq 0, \forall q,r,u$. This minimization can be performed by the standard ALS (Alternating Least Squares) algorithm, formulated as the following minimization problems [19]:

$$\mathbf{A}^{(k+1)} = \arg\min_{\mathbf{A}} \|\mathbf{Y} - \mathbf{AX}^{(k)}\|_F^2, \ s.t. \ \mathbf{A} \geq \mathbf{0}, \quad (4)$$

$$\mathbf{X}^{(k+1)} = \arg\min_{\mathbf{X}} \|\mathbf{Y}^T - \mathbf{X}^T[\mathbf{A}^{(k+1)}]^T\|_F^2, \ s.t. \ \mathbf{X} \geq \mathbf{0}. \quad (5)$$

The first step in obtaining the NMF is to acquire the set of samples. The images are given by $\bar{I}_i^N \in \mathbb{R}^{M \times N \times 3}$, where $M \times N$ is the size in pixels, with the three channels previously explained. The samples are obtained by decomposing each image in a number of square patches (i.e., non-overlapping windows). The extracted patches are of size $W \times W$ pixels

sinc(*i*) Research Center for Signals, Systems and Computational Intelligence (fich.unl.edu.ar/sinc)
P. Cavalcanti, J. Scharcanski, C. E. Martínez & L. Di Persia; "Segmentation of pigmented skin lesions using Non-negative Matrix Factorization"
In Instrumentation and Measurement Technology Conference (I2MTC) Proceedings, pp. 72-75, may, 2014.

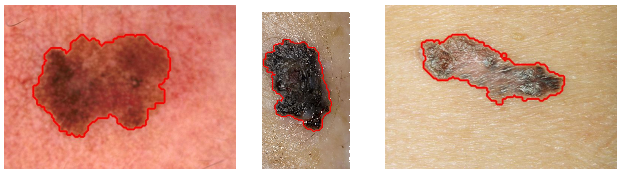

(a) (b) (c)

Fig. 1. Examples of segmentation results using $W = 5$ and $R = 1$. We superimposed the boundaries to the original images and dilated by two pixels for better visualization.

($Q = W^2 \times 3$), which are then arranged column-wise (i.e. in vectors) to form $\mathbf{Y}$.

The second step consists of the NMF calculation with the reduced rank $R$ (i.e., $R$ is the number of basis of the representation) by means of Eqs. 4 and 5. Some characteristics of the NMF approximation are more useful than others, and we cluster the activations of the bases in $\mathbf{X}$ in two clusters based on their intensity, using $k$-means. The lower activations are assigned to '0', and we only retain the most important activations in a new matrix $\hat{\mathbf{X}}$. The approximated image is reconstructed as $\hat{\mathbf{Y}} = \mathbf{A}\hat{\mathbf{X}}$, and a lesion segmentation mask is obtained by assigning to each pixel '1' if $\hat{Y}_{q,u} > 0$ (i.e. lesion pixels), and '0' otherwise.

After that, the obtained binary mask is post-processed to improve the lesion rim detection. First, we apply a morphological dilation with a disk of 5 pixels of radius, connecting neighboring small segmented regions and rounding the shape. Then, we select the largest resultant region, and perform a hole filling on it. In this way, we obtain our final segmentation result, as illustrated in Fig. 1.

## IV. Experimental Results

In our experiments, we use the same image dataset proposed by Alcón et al. [9], which contains 152 images that have been collected from the Dermnet dataset [20]. This dataset consists of 107 melanomas and 45 Clark nevi (or atypical nevi), a benign kind of lesion that present similar characteristics to melanomas. In order to evaluate the segmentation results, we used the following segmentation error criterion [4]:

$$\epsilon = \frac{Area(Segmentation \oplus GroundTruth)}{Area(GroundTruth)} \times 100\%, \quad (6)$$

where, $Segmentation$ is the result of the method in test, $GroundTruth$ is the manual segmentation of the same lesion, $Area(S)$ denotes the number of pixels indicated as lesion in the segmentation result $S$, and $\oplus$ indicates the exclusive-OR, operation that gives the pixels for which the $Segmentation$ and $GroundTruth$ disagree.

The window size $W$ and the number of NMF basis $R$ were changed to evaluate our segmentation method. The average errors obtained for all 152 processed images appear in Table I. As can be seen, the lowest average error $\epsilon$ is obtained with 1 basis and window size of $5 \times 5$.

We compared our approach with six state-of-art pigmented skin lesion segmentation methods (all discussed in Section I),

TABLE I. Average errors $\epsilon$ obtained with our proposed segmentation method.

| Window Size | 1 basis | 3 basis | 5 basis |
|---|---|---|---|
| $5 \times 5$ | **25.99%** | 28.98% | 58.02% |
| $10 \times 10$ | 27.65% | 29.77% | 40.87% |

TABLE II. Comparison of average segmentation errors $\epsilon$.

| Approach | Average $\epsilon$ |
|---|---|
| Alcón et al. Thresholding [9] | 165.31% |
| Tang's Snake [14] | 59.60% |
| Otsu's Thresh. on Grayscale [10], [11], [12] | 42.33% |
| Otsu's Thresh. on the R Channel [13] | 38.58% |
| Thresh. on a Multichannel Image [8] | 34.83% |
| ICA-Based Active-Contours [17] | 28.34% |
| **Our Proposed Method** | **25.99%** |

and the obtained average errors are shown in Table II. Considering the obtained experimental results, our proposed segmentation method provides an improved lesion rim detection for standard camera images of pigmented skin lesions.

## V. Conclusions

This paper presents a pigmented skin lesion segmentation method for standard camera images. The proposed method is based on the Non-negative Matrix Factorization of a multichannel lesion image representation. The segmentation of the lesion is then carried out by thresholding a reduced rank approximation of the original image.

The obtained results on available datasets suggest that our approach provides more accurate lesion rim detection than comparable state-of-the-art methods. Moreover, experiments also shown that only a minimum computational load of the NMF method is needed.

Future work will be devoted to STEP into the classification of the lesion type and grade. There is also a future plan to include this method in an easy-to-access pre-screening system for pigmented skin lesions.


## Acknowledgment

The authors wish to thank *Agencia Nacional de Promoción Científica y Tecnológica* (PICT 2010-1730, Argentina), *Universidad Nacional de Litoral* (CAI+D 2011 #58-511, #58-519, #58-525, Argentina), *Consejo Nacional de Investigaciones Científicas y Técnicas* (CONICET, PIP 2011 00284, Argentina), *Conselho Nacional de Desenvolvimento Científico e Tecnológico* (CNPq, Brazil), *Coordenação de Aperfeiçoamento de Pessoal de Nível Superior* (CAPES, Brazil), for their support.

C. Martínez is also with Facultad de Ingeniería, Universidad Nacional de Entre Ríos.


## References


[1] J. D. Whited, "Teledermatology research review.," *Int. J. Dermatol.*, vol. 45, no. 3, pp. 220–229, Mar 2006.

[2] World Health Organization, "How commom is skin cancer?," 2011.

[3] M. E. Celebi, H. A. Kingravi, B. Uddin, H. Iyatomi, Y. Alp Aslandogan, W. V. Stoecker, and R. H. Moss, "A methodological approach to the classification of dermoscopy images," *Comp. Med. Ima. Gra.*, vol. 31, no. 6, pp. 362 – 373, 2007.



sinc(*i*) Research Center for Signals, Systems and Computational Intelligence (fich.unl.edu.ar/sinc)
P. Cavalcanti, J. Scharcanski, C. E. Martínez & L. Di Persia; "Segmentation of pigmented skin lesions using Non-negative Matrix Factorization"
In Instrumentation and Measurement Technology Conference (I2MTC) Proceedings, pp. 72-75, may, 2014.

[4] H. Iyatomi, H. Oka, M.E. Celebi, M. Hashimoto, M. Hagiwara, M. Tanaka, and K. Ogawa, "An improved internet-based melanoma screening system with dermatologist-like tumor area extraction algorithm," *Comp. Med. Ima. Gra.*, vol. 32, no. 7, pp. 566 – 579, 2008.

[5] T. Fikrle and K. Pizinger, "Digital computer analysis of dermatoscopical images of 260 melanocytic skin lesions; perimeter/area ratio for the differentiation between malignant melanomas and melanocytic nevi.," *J Eur Acad Dermatol Venereol*, vol. 21, no. 1, pp. 48–55, Jan 2007.

[6] C. Massone, E. M. T. Wurm, R. Hofmann-Wellenhof, and H. P. Soyer, "Teledermatology: an update.," *Semin. Cutan. Med. Surg.*, vol. 27, no. 1, pp. 101–105, Mar 2008.

[7] T. Lee, V. Ng, R. Gallagher, A. Coldman, and D. McLean, "Dullrazor: A software approach to hair removal from images," *Comp in Bio and Med*, vol. 27, no. 6, pp. 533–543, November 1997.

[8] P. G. Cavalcanti and J. Scharcanski, "Automated prescreening of pigmented skin lesions using standard cameras," *Comp. Med. Ima. Gra.*, vol. In Press, Corrected Proof, pp. –, 2011.

[9] J. F. Alcon, C. Ciuhu, W. ten Kate, A. Heinrich, N. Uzunbajakava, G. Krekels, D. Siem, and G. de Haan, "Automatic imaging system with decision support for inspection of pigmented skin lesions and melanoma diagnosis," *IEEE J. Sel. Top. in Sig. Proc.*, vol. 3, no. 1, pp. 14–25, Feb. 2009.

[10] A. G. Manousaki, A. G. Manios, E. I. Tsompanaki, J. G. Panayiotides, D. D. Tsiftsis, A. K. Kostaki, and A. D. Tosca, "A simple digital image processing system to aid in melanoma diagnosis in an everyday melanocytic skin lesion unit: a preliminary report.," *Int J Dermatol*, vol. 45, no. 4, pp. 402–410, Apr 2006.

[11] D. Ruiz, V. J. Berenguer, A. Soriano, and J. Martin, "A cooperative approach for the diagnosis of the melanoma.," *Conf Proc IEEE Eng Med Biol Soc*, vol. 2008, pp. 5144–5147, 2008.

[12] K. Tabatabaie, A. Esteki, and P. Toossi, "Extraction of skin lesion texture features based on independent component analysis.," *Skin Res Technol*, vol. 15, no. 4, pp. 433–439, Nov 2009.

[13] P. Cavalcanti, Y. Yari, and J. Scharcanski, "Pigmented skin lesion segmentation on macroscopic images," in *Proc. 25th Int. Conf. Ima. Vis. Comp.*, 2010.

[14] J. Tang, "A multi-direction gvf snake for the segmentation of skin cancer images," *Pattern Recogn.*, vol. 42, pp. 1172–1179, June 2009.

[15] C. Xu and J. L. Prince, "Snakes, shapes, and gradient vector flow," *IEEE Trans. on Ima. Proc.*, vol. 7, no. 3, pp. 359–369, 1998.

[16] N. Otsu, "A threshold selection method from gray-level histograms," *IEEE Trans. Sys., Man and Cyb.*, vol. 9, no. 1, pp. 62–66, January 1979.

[17] P. G. Cavalcanti, J. Scharcanski, L. E. Di Persia, and D. H. Milone, "An ica-based method for the segmentation of pigmented skin lesions in macroscopic images," in *Proc 33rd IEEE Eng Med Biol Soc*, 2011.

[18] T. F. Chan, B. Y. Sandberg, and L. A. Vese, "Active contours without edges for vector-valued images," *J. Visual Comm. Ima. Repres.*, vol. 11, no. 2, pp. 130 – 141, 2000.

[19] A. Cichocki, R. Zdunek, A. H. Phan, and S. I. Amari, *Nonnegative matrix and tensor factorizations: applications to exploratory multiway data analysis and blind source separation*, John Wiley & Sons Ltd., United Kingdom, 2009.

[20] "Dermnet skin disease image atlas," 2009.